Title and abstract translated to Japanese

多孔質な岩石及び溶岩の破壊基準：雲仙火山溶岩ドームでの研究

マグマ(溶岩)と岩石のレオロジーと強度は，応力の蓄積と散逸を支配し，噴火様式や山体の構造的安定性に影響を与える．火山噴出物は極端に不均質であり，様々な量・サイズの結晶，ガラス(メルト)，気泡を含む．そのため，温度・応力・歪速度の関数として，その流れや亀裂形成を引き起こす状態を完全に記載することは難しい．ここで我々は，雲仙火山において溶岩ドームを形成し様々な発泡度(9-35%)を有する高結晶度(～75%)な岩石(常温)と溶岩(900度)について，その破壊を引き起こす状態を検討した．その結果，我々は岩石の強度は空隙率とともに減少し，歪速度に依存しないことを発見した：　新鮮な岩石と変質したものでは，後者でわずかに強度が大きい．また，溶岩(900°C)の強度も空隙率とともに減少する．この結果は重要なことに，脆性的振る舞いを起こす歪速度において，常温における岩石の強度は，それを900°Cまで加熱し変形させたときの強度よりも弱いことを示している．このとき，熱応力は岩石の強度に影響を与えない．

高温条件(900°C)では，溶岩のレオロジーは歪速度に強く依存する．低歪速度下($<10^{-4}$ s^{-1})では，溶岩は塑性的に振る舞い(物質が広範な固体変形を持続させる)，非ニュートン流体としてずり粘減の振る舞いを示した．このレジームでは，溶岩の見かけ粘性は，おそらく剪断時の効率的な空隙崩壊のため，発泡度に依存しない．高歪速度下($>10^{-4}$ s^{-1})では，溶岩は益々の脆性的な応答(局所的な断層に沿った破壊による変形)を示す；歪速度の関数として，強度の増加と破壊へ至るときの歪の減少が観察された．溶岩の破壊を引き起こす状態を制約するため，これら溶岩における破壊時の臨界デボラ数(De_c, 緩和時間と実験観察時間の比)を解析し，メルトにおけるそれ(De_{melt}, $=10^{-3}$-10^{-2}; Webb & Dingwell, 1990)と比較した．我々は結晶の存在がDecを2.11×10^{-4}まで減少させることを発見した．またさらに，溶岩の強度に影響する発泡度(φ)もDe_cを$-5.1\times10^{-4}\varphi+2.11\times10^{-4}$のようにコントロールする．我々はこれらの発見が与える，マグマ上昇と溶岩ドームの構造的安定性への示唆を議論する．

Supplementary Figures

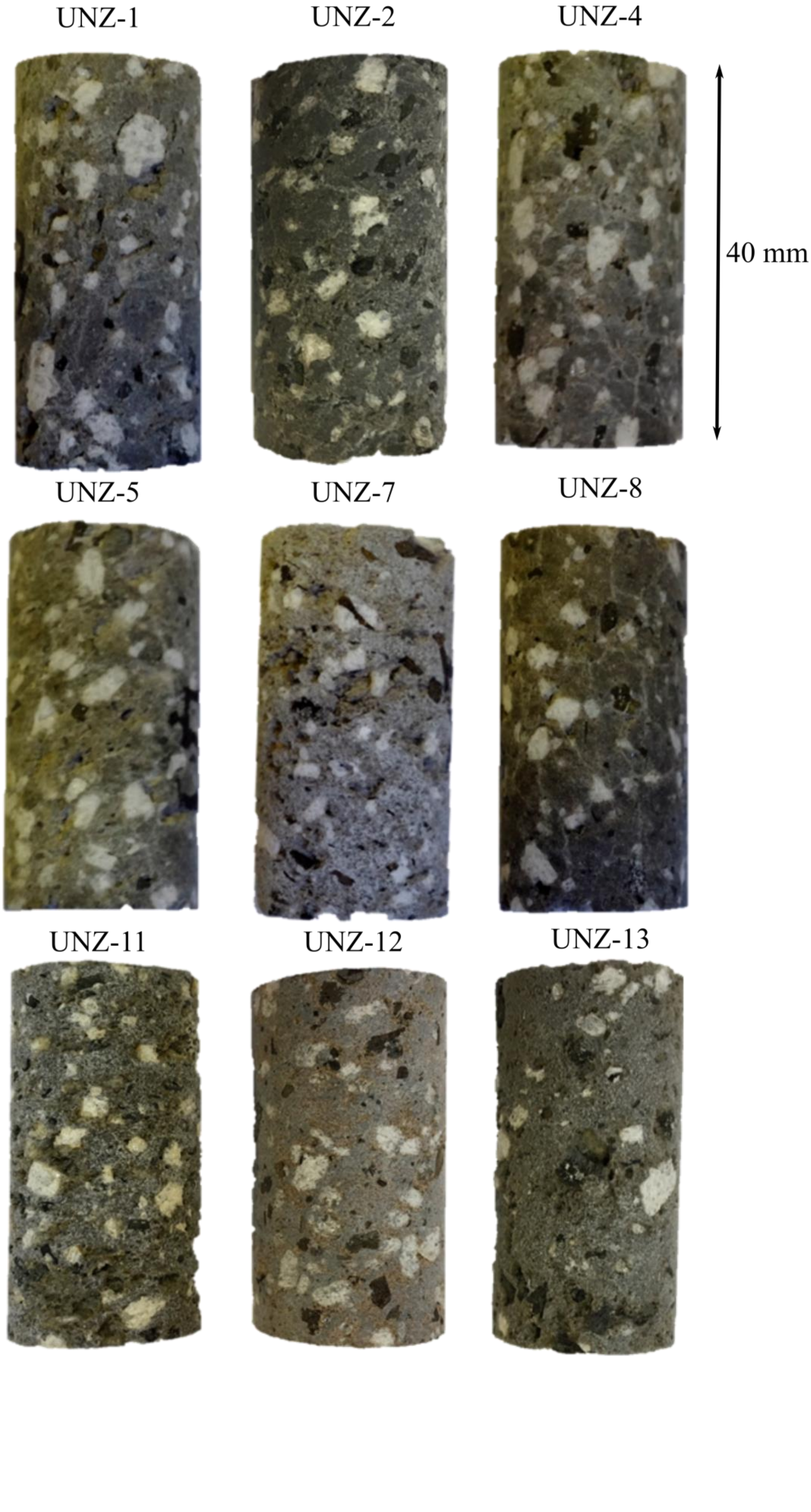

S1. Images of cores used in the uniaxial compressive stress experiments. The principal stress, σ_1, was applied in the vertical direction. In all cores large phenocrysts of plagioclase and amphibole are recognisable, as well as a network of large pores and cracks. Signs of alteration are visible in certain cores, in UNZ-11 there is a crusty white/yellowish layer around pores and overall it has a friable texture, and in UNZ-12 a reddish hue is visible.

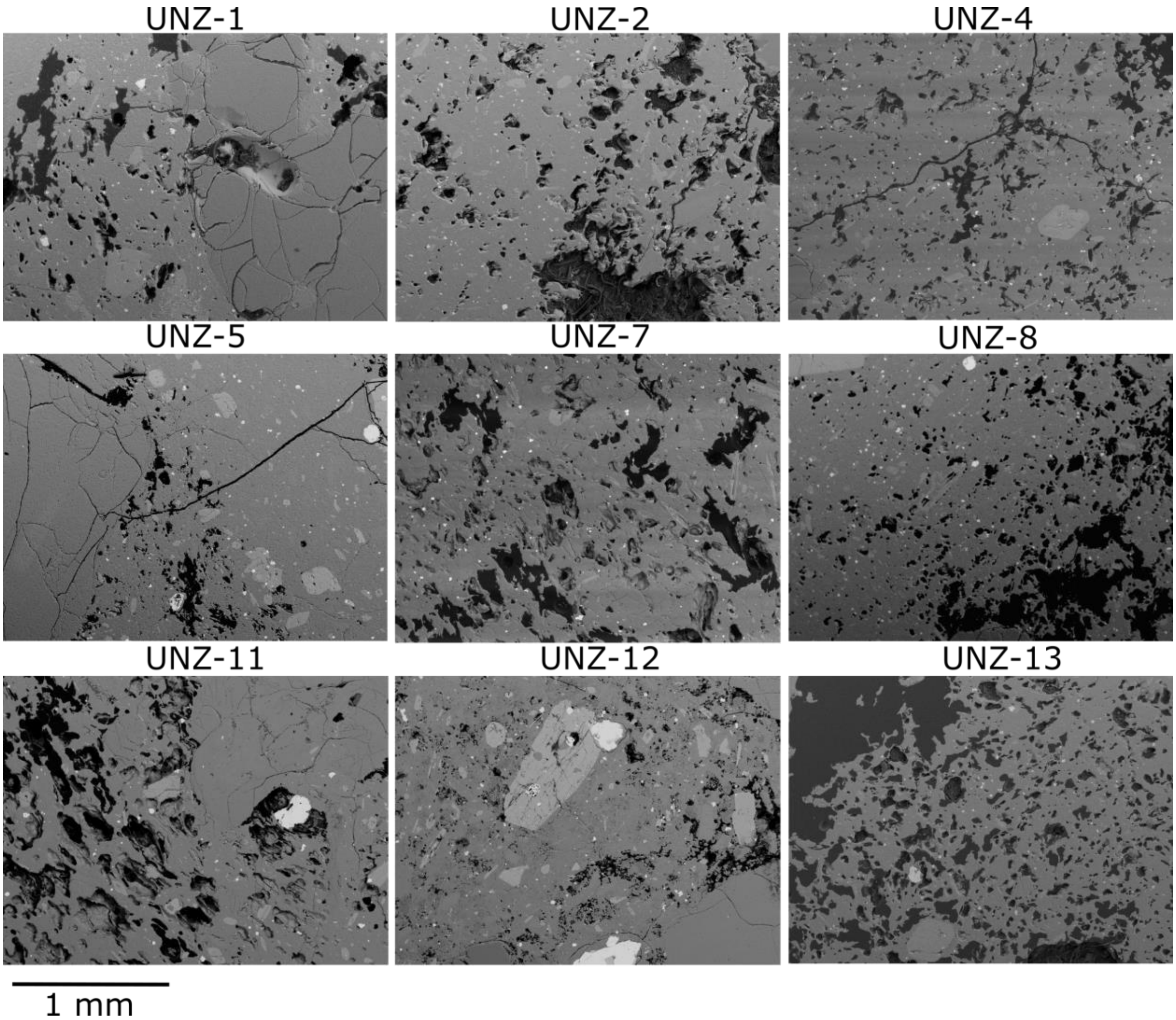

S2. Backscattered electron images of all samples used in this study. These images were taken from polished stubs and are orientated so that the later applied principal stress, $\sigma_{1,}$ was directed into the page.

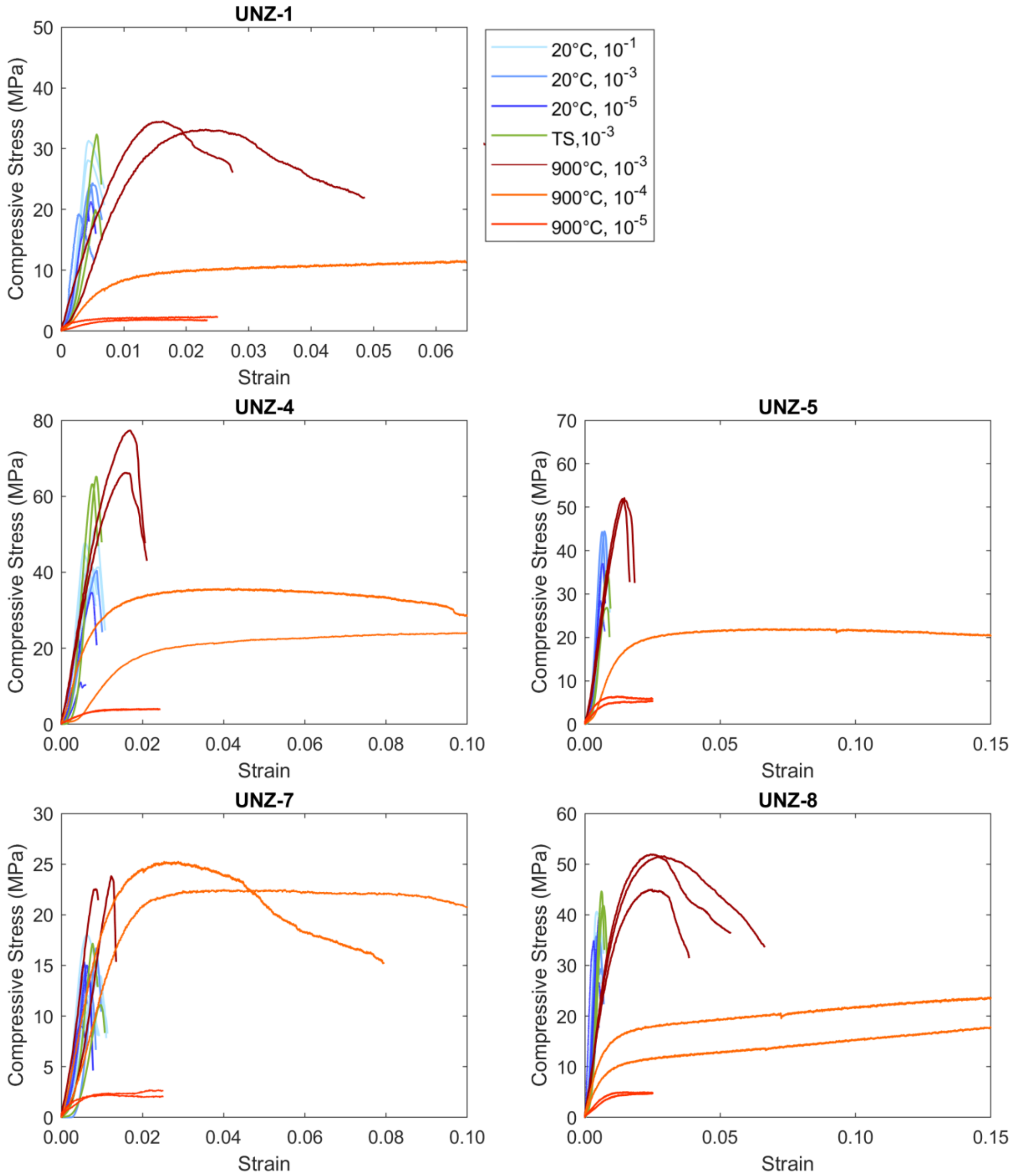

S3. Stress-strain curves for uniaxial compressive strength tests conducted on thermally stressed and pristine samples at strain rates of 10^{-1}, 10^{-3} 10^{-5} s^{-1} at ambient temperatures, and on pristine samples at strain rates of 10^{-3}, 10^{-4}, 10^{-5} s^{-1} at temperatures of 900°C. The plots are separated into block number, and therefore porosity (see Table 3). These graphs show how strength is higher at both higher porosities and at higher temperatures. Thermally treated samples do not appear to vary in strength compared to their untreated equivalents, but do show a more concave-up initial portion of the curve. Experiments carried out at higher temperature and slower strain rates, 10^{-4} and 10^{-5} s^{-1}, deform viscously in response to applied stress.

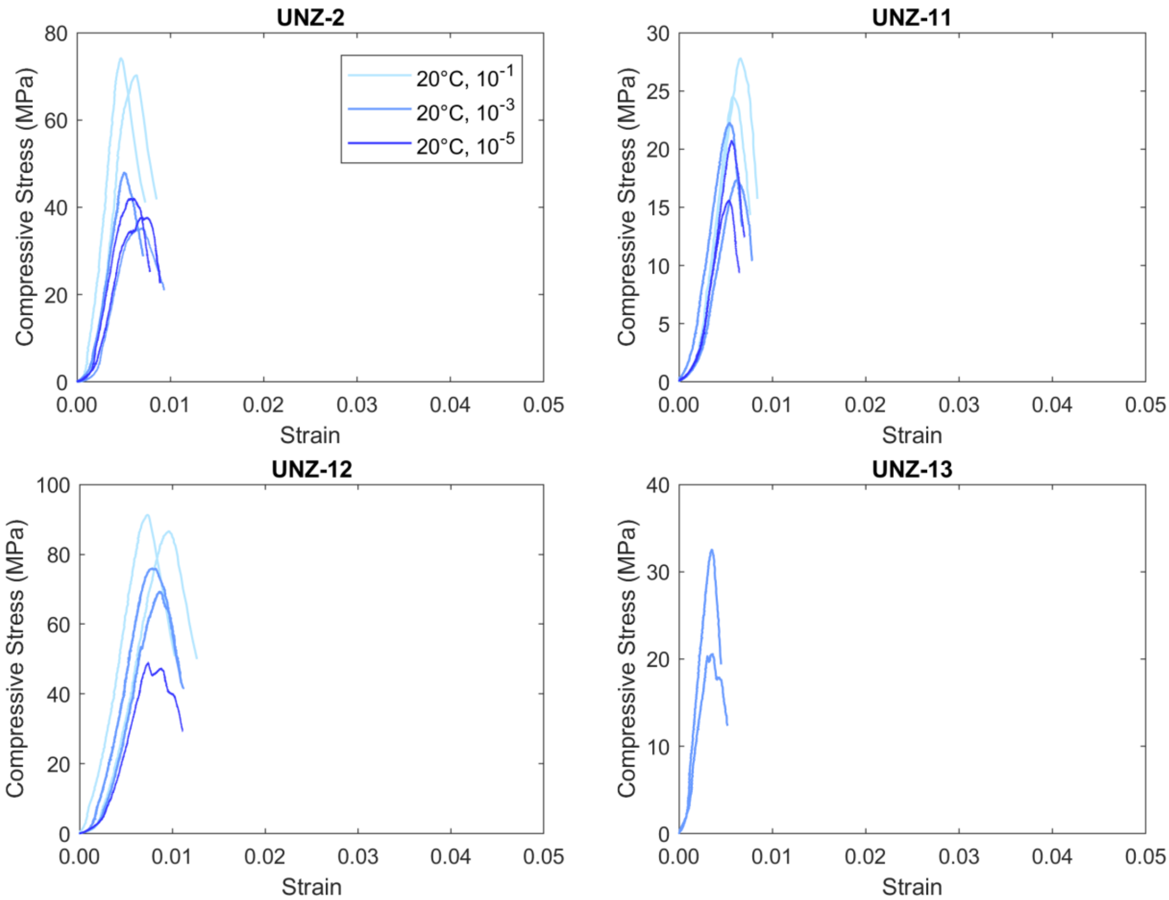

S4. Stress-strain curves for rocks deformed at strain rates of 10^{-1},10^{-3} and 10^{-5} s^{-1} at ambient temperatures only. Here the curves demonstrate that samples deformed at higher strain rates achieve higher peak stresses across the range of porosities tested.

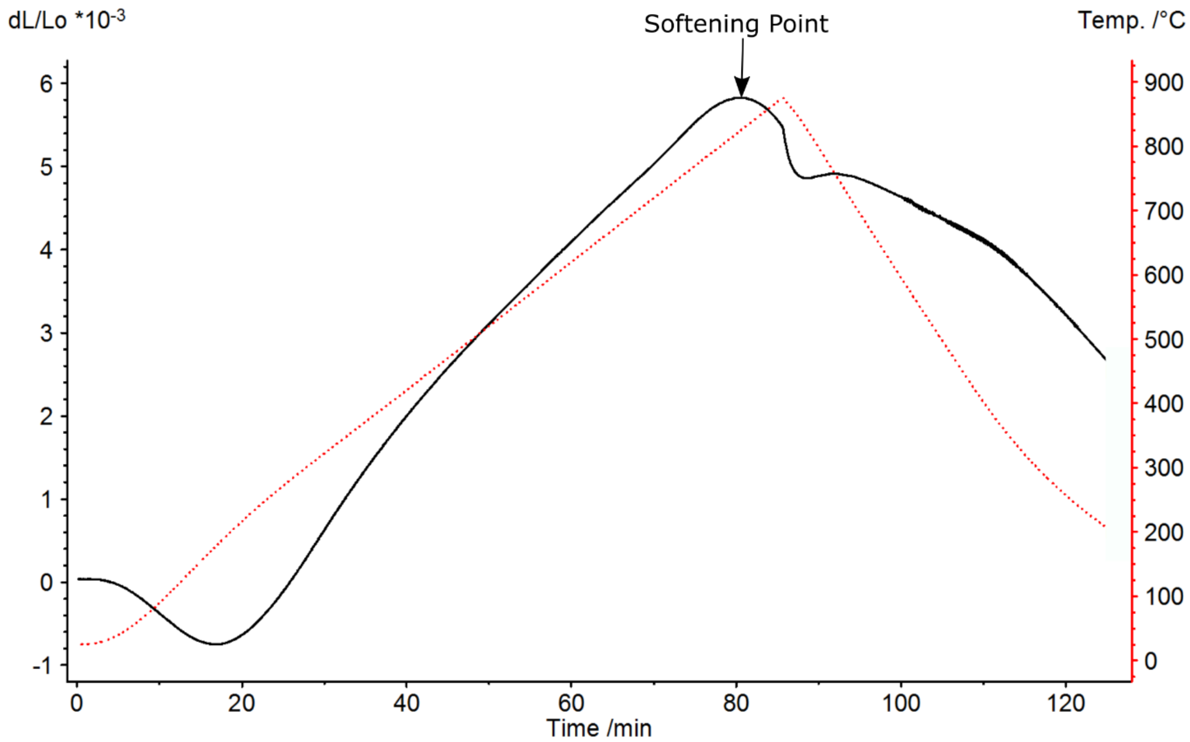

S5. Thermal analysis result showing the softening point of sample UNZ-8. The sample was heated at 10°C/min to 1100 °C whilst applying a constant load of 2N. The softening point was detected as 824.6 °C, 80.6 minutes into the experiment, when the applied load counteracted the thermal expansion of the sample, causing an inflection point (i.e. switch to contraction).

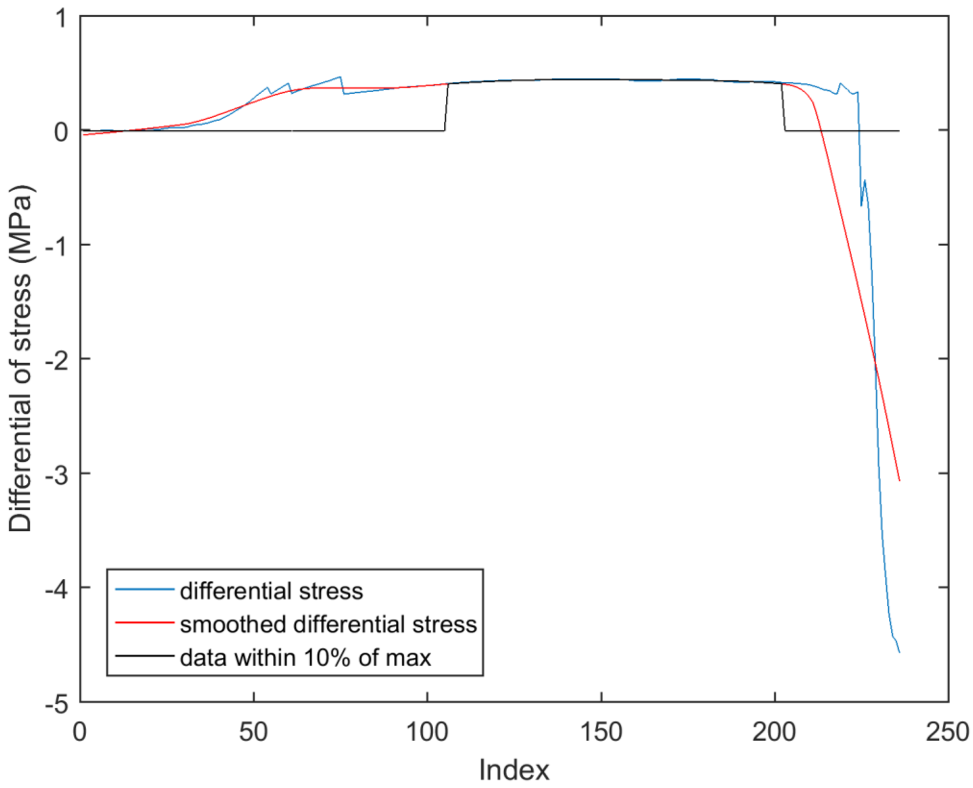

S6. Example plot (from sample UNZ-2-2) produced by the script run to find the Young's Modulus of a sample. The code looks at the gradient of the stress–strain curve and finds at which strains (the index number of the vector, x–axis) the increase in stress (y–axis) is at a maximum. The blue line shows the calculated differential of the stress, the red line is the differential stress smoothed, and the black line shows the points at which the stress is within 10 % of its maximum. The Young's modulus is then calculated with the resulting values of stress and strain from the black selector line, the maximum slope of the stress–strain curve.